

## $B_s \rightarrow K\ell\nu$ form factors with 2+1 flavors

Yuzhi Liu<sup>1</sup>, Jon A. Bailey<sup>2</sup>, A. Bazavov<sup>3</sup>, C. Bernard<sup>4</sup>, C. M. Bouchard<sup>5</sup>, C. DeTar<sup>6</sup>, Daping Du<sup>7</sup>, A. X. El-Khadra<sup>8,9</sup>, E. D. Freeland<sup>10</sup>, E. Gámiz<sup>11</sup>, Z. Gelzer<sup>8,12</sup>, Steven Gottlieb<sup>1,\*</sup>, U. M. Heller<sup>13</sup>, A. S. Kronfeld<sup>9,14</sup>, J. Laiho<sup>7</sup>, P. B. Mackenzie<sup>9</sup>, Y. Meurice<sup>12</sup>, E. T. Neil<sup>15,16</sup>, J. N. Simone<sup>9</sup>, R. Sugar<sup>17</sup>, D. Toussaint<sup>18</sup>, R. S. Van de Water<sup>9</sup>, and Ran Zhou<sup>9</sup>

<sup>1</sup>Department of Physics, Indiana University, Bloomington, Indiana 47405, USA

<sup>2</sup>Department of Physics and Astronomy, Seoul National University, Seoul, South Korea

<sup>3</sup>Department of Computational Mathematics, Science and Engineering and Department of Physics and Astronomy, Michigan State University, East Lansing, Michigan, 48824, USA

<sup>4</sup>Department of Physics, Washington University, St. Louis, Missouri, 63130, USA

<sup>5</sup>School of Physics and Astronomy, University of Glasgow, Glasgow, G12 8QQ, UK

<sup>6</sup>Department of Physics and Astronomy, University of Utah, Salt Lake City, Utah 84112, USA

<sup>7</sup>Department of Physics, Syracuse University, Syracuse, New York 13244, USA

<sup>8</sup>Department of Physics, University of Illinois, Urbana, Illinois 61801, USA

<sup>9</sup>Fermi National Accelerator Laboratory, Batavia, Illinois 60510, USA

<sup>10</sup>School of the Art Institute of Chicago, Chicago, Illinois 60603, USA

<sup>11</sup>CAFPE and Departamento de Física Teórica y del Cosmos, Universidad de Granada, Granada, Spain

<sup>12</sup>Department of Physics and Astronomy, University of Iowa, Iowa City, IA 52242, USA

<sup>13</sup>American Physical Society, Ridge, New York 11961, USA

<sup>14</sup>Institute for Advanced Study, Technische Universität München, D-85748 Garching, Germany

<sup>15</sup>Department of Physics, University of Colorado, Boulder, CO 80309, USA

<sup>16</sup>RIKEN-BNL Research Center, Brookhaven National Laboratory, Upton, NY 11973, USA

<sup>17</sup>Department of Physics, University of California, Santa Barbara, California 93106, USA

<sup>18</sup>Department of Physics, University of Arizona, Tucson, Arizona 85721, USA

**Abstract.** Using the MILC 2+1 flavor asqtad quark action ensembles, we are calculating the form factors  $f_0$  and  $f_+$  for the semileptonic  $B_s \rightarrow K\ell\nu$  decay. A total of six ensembles with lattice spacing from  $\approx 0.12$  to  $0.06$  fm are being used. At the coarsest and finest lattice spacings, the light quark mass  $m_l'$  is one-tenth the strange quark mass  $m_s'$ . At the intermediate lattice spacing, the ratio  $m_l'/m_s'$  ranges from 0.05 to 0.2. The valence  $b$  quark is treated using the Sheikholeslami-Wohlert Wilson-clover action with the Fermilab interpretation. The other valence quarks use the asqtad action. When combined with (future) measurements from the LHCb and Belle II experiments, these calculations will provide an alternate determination of the CKM matrix element  $|V_{ub}|$ .

---

\*Speaker, e-mail: sg@indiana.edu

# 1 Introduction

The Cabibbo-Kobayashi-Masakawa (CKM) matrix describes weak interaction mixing of quarks in the Standard Model of elementary particle and nuclear physics. The elements of the matrix are fundamental parameters of the Standard Model. If the CKM matrix is not unitary, or if independent determinations of a particular matrix element from different decays do not agree, that provides evidence of new physics beyond the Standard Model. The element  $|V_{ub}|$  is an important avenue to search for new physics. There is a long standing tension between its value determined from inclusive and exclusive decays. (See Figure 1.) The exclusive decay  $B \rightarrow \pi^- \ell^+ \nu$  [1] has been used to determine  $|V_{ub}|$ . The theory error from lattice calculations are smaller for the process at hand,  $B_s \rightarrow K^- \ell^+ \nu$ , because the spectator quark is strange, rather than an up or down quark. Experimental measurements of this decay will be available from LHCb and Belle II. Figure 2 shows a Feynman diagram of the decay without any of the QCD corrections that connect the valence quarks.

In this work, we use the 2+1 flavor MILC asqtad ensembles [2–4], asqtad valence light and strange quarks, and clover quarks with the Fermilab interpretation for the  $b$  quark [5]. The decay has also been studied by HPQCD [6] using MILC asqtad ensembles with HISQ light valence quarks and an NRQCD  $b$  quark. The RBC and UKQCD Collaborations [7] have used 2+1 flavor domain-wall dynamical quark ensembles, domain-wall valence light quarks and a relativistic heavy quark action for the  $b$  quark.

## 2 Matrix elements and form factors

Lattice QCD allows us to compute the hadronic matrix elements that are needed to calculate the decay amplitudes. The matrix elements can be expressed in terms of form factors in two ways:

$$\begin{aligned} \langle K(p_K) | \bar{u} \gamma^\mu b | B_s(p_{B_s}) \rangle &= \left( p_K^\mu + p_{B_s}^\mu - q^\mu \frac{M_{B_s}^2 - M_K^2}{q^2} \right) f_+(q^2) + q^\mu \frac{M_{B_s}^2 - M_K^2}{q^2} f_0(q^2) \\ &= \sqrt{2M_{B_s}} \left[ v^\mu f_{\parallel}(E_K) + p_{\perp}^\mu f_{\perp}(E_K) \right]. \end{aligned} \quad (1)$$

The initial  $B_s$ -meson 4-momentum is  $p_{B_s}$ , the final kaon 4-momentum is  $p_K$ , and the 4-momentum transfer to the leptons is  $q$ . Two form factors appear on the RHS, either  $f_+$  and  $f_0$  or  $f_{\parallel}$  and  $f_{\perp}$ . In the second expression,  $v^\mu \equiv p_{B_s}^\mu / M_{B_s}$  is the 4-velocity of the  $B_s$  meson and  $p_{\perp}^\mu \equiv p_K^\mu - (p_K \cdot v)v^\mu$  is the part of the kaon 4-momentum orthogonal to  $v$ . The vector form factor  $f_+(q^2)$  and the scalar form factor

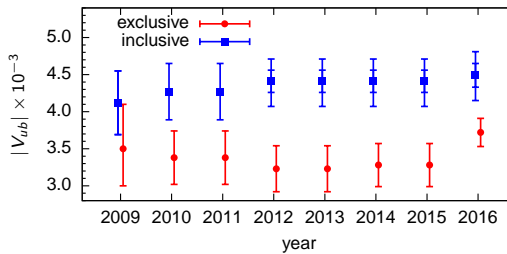


**Figure 1.** History of the tension between determination of  $|V_{ub}|$  from exclusive and inclusive decays [8].

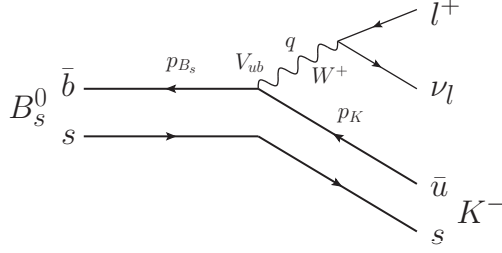


**Figure 2.** Feynman diagram for the decay  $B_s \rightarrow K^- \ell^+ \nu$  without any of the QCD corrections.

$f_+(q^2)$  satisfy the kinematic constraint  $f_+(0) = f_0(0)$ . The two sets of form factors are related by:

$$f_+(q^2) = \frac{1}{\sqrt{2M_{B_s}}} [f_{\parallel}(E_K) + (M_{B_s} - E_K)f_{\perp}(E_K)], \quad (2a)$$

$$f_0(q^2) = \frac{\sqrt{2M_{B_s}}}{M_{B_s}^2 - M_K^2} [(M_{B_s} - E_K)f_{\parallel}(E_K) + (E_K^2 - M_K^2)f_{\perp}(E_K)]. \quad (2b)$$

In lattice QCD, it is convenient to calculate the second set of form factors on each ensemble by calculating appropriate 2- and 3-point functions. The former determine the  $B_s$  meson mass, and the kaon meson mass and energy (as a function of the  $K$  3-momentum  $\mathbf{p}_K$ ). The 3-point functions determine the lattice form factors  $f_{\parallel}^{\text{lat}}$  and  $f_{\perp}^{\text{lat}}$  at the corresponding energies. After matching the currents, we obtain the continuum  $f_{\parallel}$  and  $f_{\perp}$  by performing a chiral-continuum fit and extrapolating the fit to physical quark masses and the continuum (zero lattice spacing) limit. The continuum form factors  $f_+$  and  $f_0$  are constructed from  $f_{\parallel}$  and  $f_{\perp}$  via Eqs. (2) and extrapolated to the whole kinematically allowed momentum transfer region using the  $z$ -expansion [1, 9].

### 3 Correlation functions

To carry out this calculation we need a variety of 2- and 3-point correlation functions. We define them as:

$$C_2^{B_s}(t; 0) = \sum_{\mathbf{x}} \langle O_{B_s}(t, \mathbf{x}) O_{B_s}^{\dagger}(0, \mathbf{0}) \rangle, \quad (3a)$$

$$C_2^K(t; \mathbf{p}_K) = \sum_{\mathbf{x}} \langle O_K(t, \mathbf{x}) O_K^{\dagger}(0, \mathbf{0}) \rangle e^{-i\mathbf{p}_K \cdot \mathbf{x}}, \quad (3b)$$

$$C_{3,\mu}^{B_s \rightarrow K}(t, T; \mathbf{p}_K) = \sum_{\mathbf{x}, \mathbf{y}} \langle O_K(0, \mathbf{0}) V^{\mu}(t, \mathbf{y}) O_{B_s}^{\dagger}(T, \mathbf{x}) \rangle e^{i\mathbf{p}_K \cdot \mathbf{y}}, \quad (3c)$$

where  $\mathbf{p}_K$  is the kaon momentum and  $V^{\mu}$  is the lattice vector current. The continuum vector current  $\mathcal{V}^{\mu} \equiv \bar{u} \gamma^{\mu} b = Z_{V_{\mu}} V^{\mu}$  is related to the lattice one by a renormalization factor  $Z_{V_{\mu}}$ , which is blinded until our results are finalized to avoid any bias during the analysis.

The 2-point correlators are used to extract the lattice meson masses and to verify the dispersion relation for the kaon. They also determine the overlaps of the lattice operators  $O_{B_s}$  and  $O_K$  with the  $B_s$  and  $K$  states, respectively.

## 4 Lattice details

We use six of the MILC 2+1-flavor asqtad ensembles, with lattice spacings of  $\approx 0.12, 0.09,$  and  $0.06$  fm. For each lattice spacing, we have dynamical sea quarks with mass ratio  $m'_l/m'_s = 0.1$ . For  $a \approx 0.09$  fm, we have three additional values of  $m'_l/m'_s = 0.2, 0.15$  and  $0.05$  to provide results for the chiral extrapolation. We use asqtad valence quarks. The valence  $u$  and  $d$  quarks are taken to be degenerate, and their mass  $am_l$  is the same as the light sea quark mass  $am'_l$  on the corresponding ensemble. However, the valence  $s$ -quark mass  $am_s$  is better tuned to match the physical value than the dynamical  $s$ -quark mass. This subset of the MILC ensembles was chosen based on our experience studying  $B \rightarrow \pi$  [1] and  $B \rightarrow K$  [10] semileptonic decays.

**Table 1.** Table of ensembles used and key parameters. From left to right: approximate lattice spacing; grid size; sea light and strange quark masses in lattice units; valence strange quark masses in lattice units; number of configurations analyzed; number of different time sources used on each ensemble; product of pion mass and spatial size.

$\approx a(\text{fm})$	$N_s^3 \times N_t$	$am'_l/am'_s$	$am_s$	$N_{\text{config}}$	$N_{\text{source}}$	$aM_\pi N_s$
0.12	$24^3 \times 64$	0.0050/0.0500	0.0336	2099	4	3.8
0.09	$28^3 \times 96$	0.0062/0.031	0.0247	1931	4	4.1
0.09	$32^3 \times 96$	0.00465/0.031	0.0247	1015	8	4.1
0.09	$40^3 \times 96$	0.0031/0.031	0.0247	1015	8	4.2
0.09	$64^3 \times 96$	0.00155/0.031	0.0247	791	4	4.8
0.06	$64^3 \times 144$	0.0018/0.018	0.0177	827	4	4.3

The 2-point correlators are fit to these functional forms:

$$C_2^{B_s}(t; 0) = \sum_{n=0}^{2N-1} (-1)^{n(t+1)} \frac{|\langle 0 | \mathcal{O}_{B_s} | B_s^{(n)} \rangle|^2}{2M_{B_s}^{(n)}} \left( e^{-M_{B_s}^{(n)} t} + e^{-M_{B_s}^{(n)} (N_t - t)} \right), \quad (4a)$$

$$C_2^K(t; \mathbf{p}_K) = \sum_{n=0}^{2N-1} (-1)^{n(t+1)} \frac{|\langle 0 | \mathcal{O}_K | K^{(n)} \rangle|^2}{2E_K^{(n)}} \left( e^{-E_K^{(n)} t} + e^{-E_K^{(n)} (N_t - t)} \right). \quad (4b)$$

We use  $N = 3$  in our fits, with prior central values for  $n = 0$  based on effective masses. We have set the prior widths widely enough to avoid bias. We fit over the  $t$  range  $[t_{\min}, t_{\max}]$ , with  $t_{\min}$  selected so that the fit has a good  $p$ -value and the ground state energy is stable under variations in  $t_{\min}$ . We choose  $t_{\max}$  so that the fractional error in the correlator is  $< 3\%$ , thereby ignoring any noisy tail at large  $t$ . We use kaon 3-momentum up to  $(1, 1, 1) \times 2\pi/N_s$  in lattice units, and have verified that the energy-momentum dispersion relation is well satisfied.

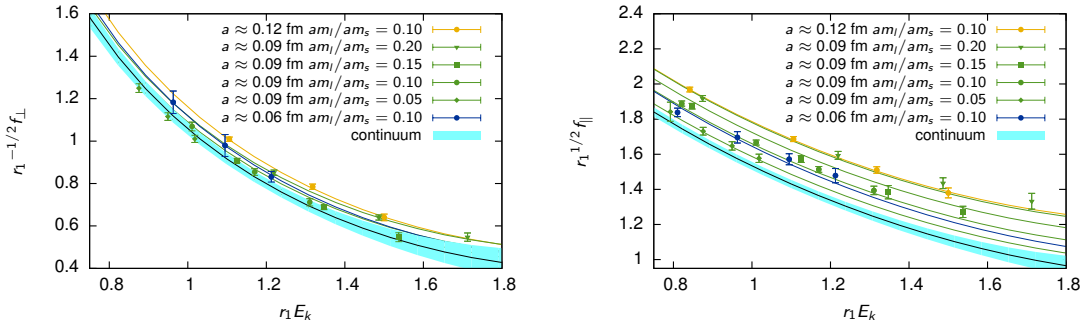
The 3-point correlators are described by

$$C_{3,\mu}^{B_s \rightarrow K}(t, T; \mathbf{p}_K) = \sum_{m,n=0}^{2N-1} (-1)^{m(t+1)} (-1)^{n(T-t-1)} A_{mn}^\mu e^{-E_K^{(m)} t} e^{-M_{B_s}^{(n)} (T-t)}, \quad (5)$$

where

$$A_{mn}^\mu = \frac{\langle 0 | \mathcal{O}_K | K^{(m)} \rangle \langle K^{(m)} | V^\mu | B_s^{(n)} \rangle \langle B_s^{(n)} | \mathcal{O}_{B_s} | 0 \rangle}{2E_K^{(m)} 2M_{B_s}^{(n)}}. \quad (6)$$

Since the energies and amplitudes are common to 2- and 3-point functions, it is possible to fit them simultaneously. An example of this fit for  $a \approx 0.12$  fm can be found in Ref. [11], Figure 2.



(a)  $f_{\perp}$  data and fit lines for each ensemble.  $f_{\parallel}$  and  $f_{\perp}$  are fit simultaneously. The cyan band shows the continuum limit.

(b)  $f_{\parallel}$  data and fit lines for each ensemble.

**Figure 3.** Chiral-continuum fit to the lattice form factors. These form factors are blinded, *i.e.*, the person doing the analysis is given the current renormalizations, but they have been multiplied by a blinding factor only known to the person supplying the renormalizations. Only after the analysis is complete will the blinding factor be revealed so that the form factors can be properly normalized.

## 5 Chiral-continuum extrapolation

Having extracted the lattice form factors on each ensemble for several values of  $E_K$ , we are ready to perform the chiral-continuum fit. We do this using SU(2) heavy-meson rooted-staggered chiral perturbation theory (HM $\chi$ P) [10, 12, 13]. At next to leading order, each form factor  $f_P$  is fit to the form

$$f_{P,\text{NLO}} = f_P^{(0)} [c_P^0 (1 + \delta f_{P,\text{logs}}) + c_P^1 \chi + c_P^2 \chi^2 + c_P^3 \chi E + c_P^4 \chi E^2 + c_P^5 \chi a^2], \quad (7)$$

where the leading order term  $f_P^{(0)}$  is

$$\frac{1}{f_P} \frac{g_{\pi}}{E_K + \Delta_P^*}. \quad (8)$$

There is a pole determined by  $\Delta_P^*$  which takes the form

$$\Delta_P^* = \frac{M_{B^*}^2 - M_{B_s}^2 - M_K^2}{2M_{B_s}}. \quad (9)$$

We require  $f_{\parallel}$  and  $f_{\perp}$  to have the same pole as  $f_0$  and  $f_+$ , respectively. This is reasonable because, by Eq. (2)  $f_{\parallel}$  and  $f_{\perp}$  are dominated by contributions from  $f_0$  and  $f_+$ , respectively. The vector meson (with  $J^P = 1^-$ ) has been experimentally measured [8] as  $M_{B^*} = 5324.65(25)$  MeV. The scalar  $B^*$  meson (with  $J^P = 0^+$ ) has not been observed experimentally, but a lattice QCD calculation [14] suggests the mass difference between  $0^+$  and  $0^-$  states to be around 400 MeV, *i.e.*  $M_{B^*}(0^+) - M_B \approx 400$  MeV. The  $J^P = 1^-$  pole is below the  $B\pi$  production threshold, while the  $0^+$  one is slightly above it, but still has a significant influence on the shape of the form factor. The  $c_P^i$  are coefficients of the corrections that depend on quark masses, kaon energy, square of kaon energy, and square of lattice spacing. They are fit parameters. Details of the chiral logarithms can be found in [10].

For our central fit of  $f_{\parallel}$  and  $f_{\perp}$  we allow additional NNLO analytic terms [1], fitting both form factors simultaneously. Figure 3 shows the result of our fit. We note that  $\chi^2/\text{dof} = 0.89$  with 42 degrees of freedom corresponding to a  $p$ -value of 0.68.

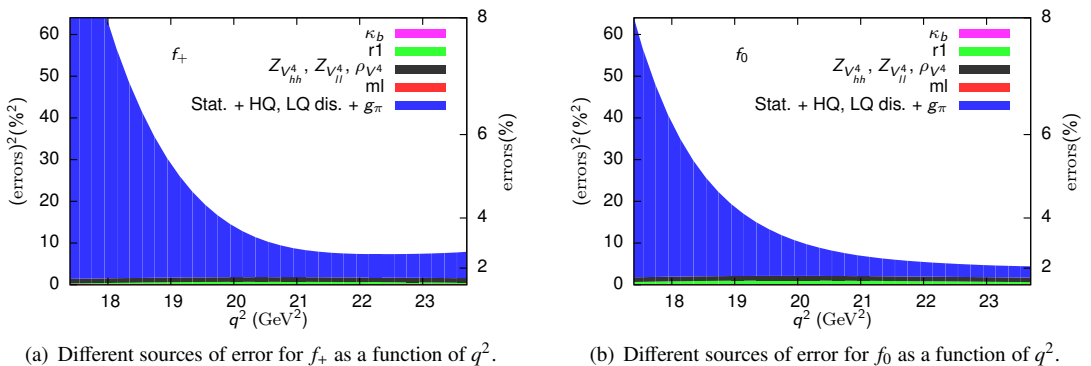


**Figure 4.** Error budgets from statistical and systematic effects.

There are several other sources of systematic error that must also be taken into account. These include tuning of  $\kappa_b$  needed to get the right  $b$ -quark mass, possible mistuning of  $am_l'$  from its physical value  $am_l$ , uncertainty in the physical value of  $r_1$  [15], and the uncertainty in the renormalization of the vector current. The quantity  $r_1$  is related to the static potential and a variation on the Sommer scale [16]. It is discussed extensively in Ref. [4], Sec. IV.B. Discretization effects from the light and heavy quark actions and errors in the coupling  $g_\pi$  needed for the chiral logarithms are combined with the statistical errors because they are parameters in the chiral-continuum fit. At this point, we use Eq. (2) to convert from the lattice form factors to  $f_+$  and  $f_0$ . In Fig. 4, we show our *preliminary* error budgets. Note that the statistical errors dominate the systematic errors, and they grow rapidly as  $q^2$  decreases.

To reduce errors and extrapolate to  $q^2 < 17\text{GeV}^2$ , we use the functional  $z$ -expansion method described in Ref. [1]. This avoids construction and fitting of synthetic data. For the  $z$ -expansion, we use the so-called BCL approach first described in Ref. [9]. We fit  $f_+$  and  $f_0$  simultaneously keeping terms up to order  $z^3$  without imposing the kinematic constraint  $f_+(q^2 = 0) = f_0(q^2 = 0)$ . We see in Fig. 5 that this condition is well satisfied as  $q^2 = 0$  corresponds to the maximum value of  $z$  in the figure. We also note that the unitarity condition  $\sum_{m,n=0}^K B_{mn} b_m b_n \leq 1$  is well satisfied by our fit. The sums are 0.160(30) for  $f_+$  and 0.157(45) for  $f_0$ . Imposition of constraints from heavy quark effective theory or kinematics would only slightly reduce the error in the form factors at  $q^2 = 0$ . Our  $z$ -expansion fit has  $\chi^2/dof = 0.82$  for 5 degrees of freedom which corresponds to a  $p$ -value of 0.54. We next reconstruct the form factors as functions of  $q^2$ . Our preliminary result, for which the  $Z$  factors for current renormalization are still blinded, is shown in Fig. 6.

## 6 Summary

This paper contains an update on our lattice QCD calculation of the form factors  $f_+$  and  $f_0$  for the decay  $B_s \rightarrow K\ell\nu$ . Our results are still preliminary. Once we finalize the systematic error analysis, we will unblind the form factors, and compare them to previous results. Before unblinding, we can only predict the shape of the decay distribution, not its absolute magnitude. Once we unblind, we can use existing information about  $|V_{ub}|$  to predict the  $B_s$  differential decay rate. Alternatively, once the decay distribution is experimentally measured, our form factors can be used to infer  $|V_{ub}|$  from this decay. This may shed light on the current discrepancy between exclusive and inclusive modes.

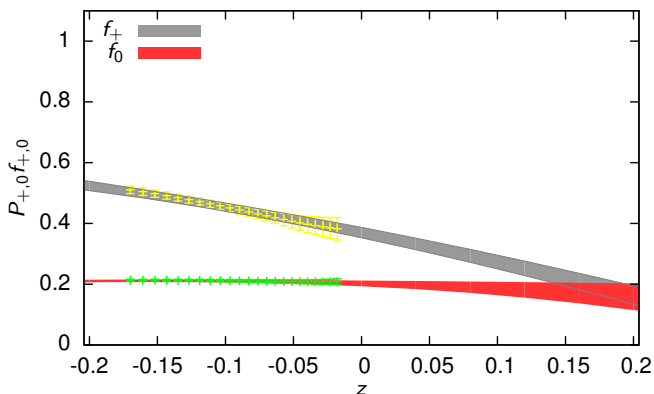


**Figure 5.** Blinded form factors as a function of  $z$ . The region in which there is lattice data is shown with its errors in yellow for  $f_+$  and green for  $f_0$ .

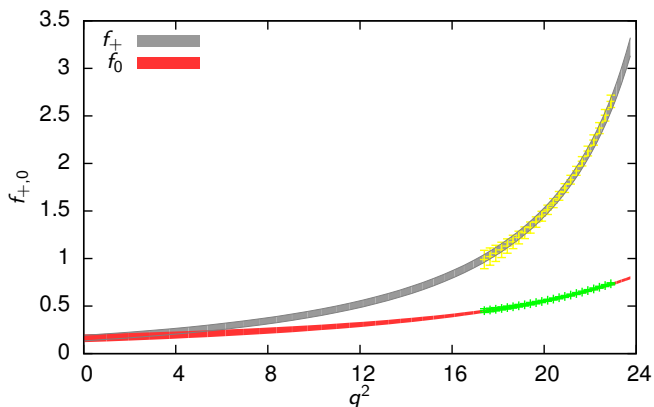


**Figure 6.** Blinded form factors shown in previous figure are now plotted vs.  $q^2$ . Color scheme is the same as before.

**Acknowledgments:** Computations for this work were carried out with resources provided by the USQCD Collaboration, the National Energy Research Scientific Computing Center and the Argonne Leadership Computing Facility, which are funded by the Office of Science of the U.S. Department of Energy; and with resources provided by the National Institute for Computational Science and the Texas Advanced Computing Center, which are funded through the National Science Foundation's Teragrid/XSEDE Program.

This work was supported in part by the U.S. Department of Energy under grants No. DE-AC05-06OR23177 (B.C.), No. DE-SC0010120 (S.G.), No. DE-SC0015655 (A.X.K.), No. DE(-)SC0009998 (J.L.), No. DE(-)SC0010113 (Y.M.), No. DE-SC0010005 (E.T.N.), No. DE-FG02-13ER41976 (D.T.), by the U.S. National Science Foundation under grants PHY14-17805 (D.D., J.L.), PHY12-12389 (Y.L.), PHY14-14614 (C.D.), and PHY13-16748 and PHY16-20625 (R.S.); by the Fermilab Distinguished Scholars Program (A.X.K.); by the German Excellence Initiative and the European Union Seventh Framework Program under grant agreement No. 291763 as well as the Eu-

ropean Union's Marie Curie COFUND program (A.S.K.), and by Spanish MINECO under grant No. FPA2013-47836-C3-1-P (E.G.). Y.L. was partially supported by the Blue Waters PAID program. The Blue Waters sustained-petascale computing project, which is supported by the National Science Foundation (awards OCI-0725070 and ACI-1238993) and the state of Illinois. Blue Waters is a joint effort of the University of Illinois at Urbana-Champaign and its National Center for Supercomputing Applications.

Fermilab is operated by Fermi Research Alliance, LLC, under Contract No. DE-AC02-07CH11359 with the United States Department of Energy, Office of Science, Office of High Energy Physics. The United States Government retains and the publisher, by accepting the article for publication, acknowledges that the United States Government retains a non-exclusive, paid-up, irrevocable, world-wide license to publish or reproduce the published form of this manuscript, or allow others to do so, for United States Government purposes.

## References

- [1] J.A. Bailey et al. (Fermilab Lattice, MILC), *Phys. Rev.* **D92**, 014024 (2015), 1503.07839
- [2] C.W. Bernard, T. Burch, K. Orginos, D. Toussaint, T.A. DeGrand, C.E. Detar, S. Datta, S.A. Gottlieb, U.M. Heller, R. Sugar, *Phys. Rev.* **D64**, 054506 (2001), hep-lat/0104002
- [3] C. Aubin, C. Bernard, C. DeTar, J. Osborn, S. Gottlieb, E.B. Gregory, D. Toussaint, U.M. Heller, J.E. Hetrick, R. Sugar, *Phys. Rev.* **D70**, 094505 (2004), hep-lat/0402030
- [4] A. Bazavov et al. (MILC), *Rev. Mod. Phys.* **82**, 1349 (2010), 0903.3598
- [5] A.X. El-Khadra, A.S. Kronfeld, P.B. Mackenzie, *Phys. Rev. D* **55**, 3933 (1997)
- [6] C.M. Bouchard, G.P. Lepage, C. Monahan, H. Na, J. Shigemitsu, *Phys. Rev.* **D90**, 054506 (2014), 1406.2279
- [7] J.M. Flynn, T. Izubuchi, T. Kawanai, C. Lehner, A. Soni, R.S. Van de Water, O. Witzel, *Phys. Rev.* **D91**, 074510 (2015), 1501.05373
- [8] C. Patrignani et al. (Particle Data Group), *Chin. Phys.* **C40**, 100001 (2016)
- [9] C. Bourrely, I. Caprini, L. Lellouch, *Phys. Rev.* **D79**, 013008 (2009), [Erratum: *Phys. Rev.*D82,099902(2010)], 0807.2722
- [10] J.A. Bailey et al., *Phys. Rev.* **D93**, 025026 (2016), 1509.06235
- [11] Y. Liu et al., *PoS LATTICE2013*, 386 (2014), 1312.3197
- [12] C. Aubin, C. Bernard, *Phys. Rev. D* **73**, 014515 (2006)
- [13] C. Aubin, C. Bernard, *Phys. Rev. D* **76**, 014002 (2007)
- [14] E.B. Gregory et al., *Phys. Rev.* **D83**, 014506 (2011), 1010.3848
- [15] A. Bazavov et al. (Fermilab Lattice, MILC), *Phys. Rev.* **D85**, 114506 (2012), 1112.3051
- [16] R. Sommer, *Nucl. Phys.* **B411**, 839 (1994), hep-lat/9310022